III

The fractional asymmetry given by (16), for Møller scattering, is plotted in Figs. 4 and 5. An absolute maximum in $P(p,\vartheta)$ occurs near $p/m=1.0$ (i.e., $E_{\text{lab-kin}} \approx 1.0$ Mev), and $\vartheta=60°$. Figure 4 shows the angular dependence of $P$ at the maximal value of $p/m$ and Fig. 5 shows the energy dependence at the maximal value of $\vartheta$.

If (15) is applied to the scattering of $\mu$ mesons on a polarized electron target, we obtain numbers of the same order of magnitude as in the case of Møller scattering. In the more realistic case (since hydrogen electrons are not easily polarized) of the scattering of transversally polarized $\mu$ mesons on unpolarized electrons, the value of $P$ is more than an order of magnitude smaller.

PHYSICAL REVIEW VOLUME 120, NUMBER 5 DECEMBER 1, 1960

# Positive Pion Production in $p$-$p$ Collisions at 420 Mev with Polarized Protons*†

ROBERT H. MARCH‡§
*The Enrico Fermi Institute for Nuclear Studies and The Physics Department, The University of Chicago, Chicago, Illinois*
(Received July 25, 1960)

The asymmetry in the production of positive $\pi$ mesons in $p$-$p$ collisions has been studied, using a 420-Mev, 62% polarized proton beam from the Chicago synchrocyclotron, with nuclear emulsions as the pion detector. The asymmetry at 65° in the laboratory for the entire spectrum above 20 Mev in the center-of-mass system is found to be $0.151\pm0.021$, in the direction opposite the elastic scattering that produced the polarized beam. In the region of the spectrum above 40 Mev, results are consistent with those found by other authors for the reaction $p+p\rightarrow\pi^+ +d$; at lower energies where pions associated with final nucleon $p$ states become predominant, the asymmetry decreases rapidly and may possibly reverse.

## I. INTRODUCTION

THE asymmetry of positive pion production in the reaction

$$p+p\rightarrow\pi^+ +d, \tag{1}$$

with polarized protons, predicted by Marshak and Messiah[1] from the phenomenological theory of Brueckner and Watson,[2] has been studied by a number of authors.[3] Until recently the only results available[4] on the asymmetry of pions from the reaction

$$p+p\rightarrow\pi^+ +n+p \tag{2}$$

seemed to indicate an opposite asymmetry for this reaction, though recent results by McIlwain *et al.*[5] on about 250 events seem to indicate that this result was spurious. A reversed asymmetry in reaction (2) would be surprising in view of the fact that the angular momentum states that account for reaction (1) are also responsible for the bulk of the spectrum of reaction (2), and this experiment was undertaken to resolve this conflict with the phenomenological theory.

Because of the low cross section for reaction (2), the pion detector must be stable over long periods of time, of high efficiency and solid angle, view the entire spectrum simultaneously, and have a high rejection of spurious background events, with certain identification of positive pions and reasonable energy resolution. Nuclear emulsions insensitive to minimum ionizing particles (Ilford *GB*)[6] possess these features and, in addition, permit internal checks on the beam polarization and the geometric alignment of the apparatus. The emulsions may be area-scanned for pion endings, the pion being identified by its decay and its energy determined from its range. It was felt that results obtained by this technique, though limited in statistical accuracy, might be more convincing than those obtained with the relatively intricate counter telescope that would be required to perform this experiment with counters.

## II. APPARATUS AND PROCEDURE

### A. The Polarized Proton Beam

The beam was produced by scattering the internal beam of the Chicago synchrocyclotron 13° to the left in a beryllium target, emerged through a magnetic channel, and entered the exit system used with the external proton beam,[7] as shown in Fig. 1. Target

* A thesis submitted to the Department of Physics, the University of Chicago, in partial fulfillment of the requirements for the Ph.D. degree.

† Research supported by a joint program of the Office of Naval Research and the U. S. Atomic Energy Commission.

‡ Shell Oil Company Fellow, 1957–1958.

§ Now at the University of Wisconsin, Madison, Wisconsin.

[1] R. E. Marshak and A. M. L. Messiah, Nuovo cimento **11**, 337 (1954). See also reference 17.

[2] K. M. Watson and K. A. Brueckner, Phys. Rev. **83**, 1 (1951).

[3] T. H. Fields, J. G. Fox, J. A. Kane, R. A. Stallwood, and R. B. Sutton, Phys. Rev. **109**, 1704 (1958); F. S. Crawford and M. L. Stevenson, Phys. Rev. **97**, 1305 (1955).

[4] H. G. de Carvalho, E. Heiberg, J. Marshall, and L. Marshall, Phys. Rev. **94**, 1796 (1954).

[5] R. McIlwain, J. Deahl, M. Derrick, J. Fetkovich, and T. Fields, Bull. Am. Phys. Soc. **4**, 23 (1959).

[6] A. H. Rosenfeld, Phys. Rev. **96**, 130 (1954).

[7] A. V. Crewe and U. E. Kruse, Rev. Sci. Instr. **27**, 5 (1956).

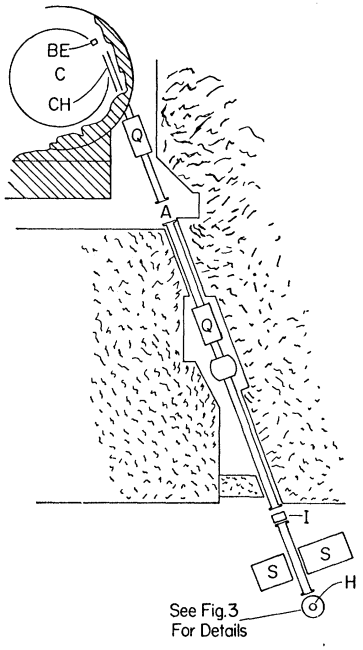


FIG. 1. Plan view of beam extraction and focussing. (*C*)—Cyclotron; (*BE*)—Beryllium target; (*CH*) — Magnetic channel; (*A*)—Air gap for focussing measurements; (*Q*)—Quadrupole magnets; (*I*)—Ionization chamber; (*S*)—Shielding; (*H*)—Hydrogen target.

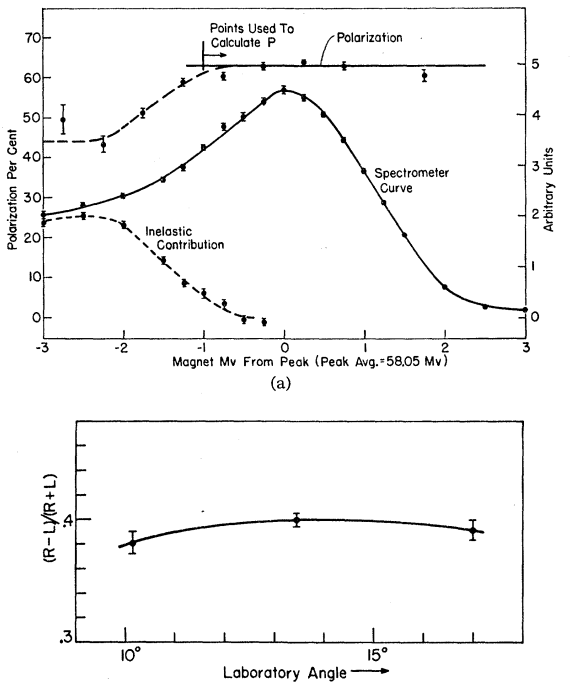


FIG. 2. (a) Combined (right+left) momentum spectrum, in arbitrary units, of protons scattered from beryllium at 13°, and polarization as a function of momentum calculated from this measurement. The inelastic contribution is estimated by subtracting the momentum spectrum of the unscattered beam. (b) Angular dependence of the asymmetry of the second scattering in beryllium.

position and scattering angle were fixed on the basis of orbit tracing in the channel and exit pipe, using a tensioned current-carrying wire. The channel, designed by Kruse, has been previously used[8] to extract a polarized beam in different geometry.

The beam flux was approximately $10^7$ protons per second and was focussed in the target area to a spot approximately $\frac{1}{2}$ inch wide and $\frac{3}{4}$ inch high at half maximum intensity.

The mean energy was 419.8±0.7 Mev, as determined by the standard Bragg-curve technique[9] in a copper absorber, with an energy spread of 7.1-Mev standard deviation, as measured with a high-resolution magnetic spectrometer[10] designed by A. V. Crewe.

The polarization was 0.624±0.011, as determined from the asymmetry of a second scattering in beryllium, analyzed by the Crewe spectrometer. Momentum spectra of scattered protons were then taken at equal angles on both sides of the beam. At frequent intervals, the beam center was determined by transits of the spectrometer magnet across the beam. These transits were internally consistent to ±0.05°.

The combined $(R+L)$ spectrum for a scattering angle of 13°, is shown in Fig. 2(a), along with the polarization $[(R-L)/(R+L)]$[8]. The inelastic second-scattering contribution is estimated by subtracting from the observed spectrum a spectrum obtained with the magnet viewing the beam directly. The absence of any appreciable momentum dependence of the asymmetry above the maximum momentum of inelastic second scattering indicates that the beam probably originates primarily from elastic first scattering. It is felt that this feature of the polarization measurement technique permits a confidence in the polarization value not possible with the conventional range-telescope technique of detecting the second scattering.

The portion of the spectrum used to obtain the quoted polarization is indicated in Fig. 2(a). Inclusion of the entire curve gives a lower limit value of 0.59 for the polarization. As the beam exit channel accepts particles up to about one degree from the central scattering angle, the angular dependence of the asymmetry was checked [Fig. 2(b)] by taking spectra at two adjoining angles and proved negligible over this small range. The quoted error contains allowances for uncertainty in the energy dependence of the polarization, beam center angle, and first scattering angle, in addition to statistical errors.

An internal check on the beam polarization was obtained by counting elastically scattered protons stopping in the emulsion, which showed an asymmetry of 0.258±0.028. Using the $p$-$p$ polarization data of Kane *et al.*,[11] this gives a value of 0.66±0.08 for the beam polarization.

[8] E. Heiberg, Phys. Rev. **106**, 1271 (1957).
[9] R. L. Mather and E. Segrè, Phys. Rev. **84**, 181 (1951).
[10] A. V. Crewe, Rev. Sci. Instr. **29**, 880 (1958).
[11] J. A. Kane, R. B. Sutton, R. A. Stallwood, J. G. Fox, and T. H. Fields, Phys. Rev. **95**, 1694 (1954).

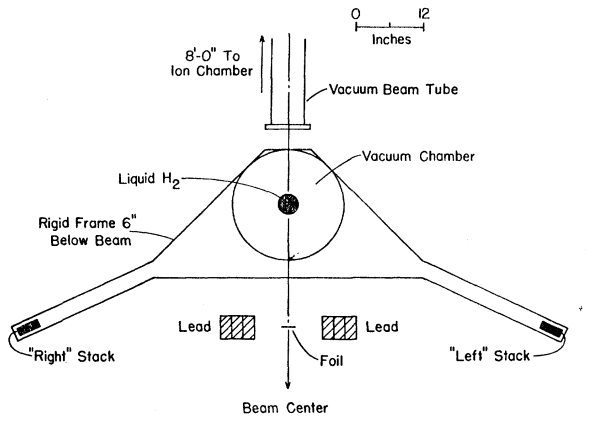


FIG. 3. Plan view of emulsions, target, monitor foil, and related apparatus.

## B. Target and Exposure Geometry

Figure 3 shows the target and emulsions in plan view. The emulsion stacks were exposed at an angle of 64.7°. This angle was selected to give center-of-mass angles close to 90°, at which the asymmetry is at a maximum and can be measured independently of the differential cross section, without going far enough forward in the laboratory to obscure a significant portion of the pion spectrum in the high background of elastically scattered protons, about 50 times more numerous than the pions at these angles and energies. The emulsion stacks each contained fourteen 4-in.×3-in.×1900 micron pellicles, with the long edge vertical and facing the target, clamped with 1.2 cm of old unexposed emulsion at either end to insure a medium of equal stopping power.

The target,[12] kindly lent by Kruse, was a 3.75-in. diameter Mylar-walled cylinder containing liquid hydrogen at atmospheric pressure and surrounded by a 20-in. diameter vacuum chamber with 0.012-in. aluminum walls. Target thickness was 0.68 g/cm² of hydrogen.

Target and emulsion holders were fixed to a prealigned frame. The angular alignment of the emulsions could be checked by taking advantage of the rapid variation of energy with angle for elastically scattered protons in this angular region. Figure 4(a) shows the variation of proton range across each stack; a least-squares fit to straight lines of equal slope indicates a difference in angle between the two stacks, $(\theta_R-\theta_L)=-0.02°\pm0.10°$, which is too small to significantly affect the pion asymmetry. Centering of the beam in the apparatus was checked by monitoring the beam profile throughout the exposure with a nichrome foil. The activation of vertical strips of the foil was checked 24 hours after the exposure to permit decay of short-lived activities and thereby obtain a beam profile integrated over the exposure time. Figure 4(b) shows the beam profile thus obtained. From this profile, it can be calculated that the "false asymmetry" of solid angle due to beam miscentering was $(\Omega_R-\Omega_L)/(\Omega_R+\Omega_L)=0.0003\pm0.0031$, negligible within the accuracy of this experiment.

[12] U. E. Kruse and R. C. Arnold, Enrico Fermi Institute of Nuclear Studies report EFINS-332, 1960 (unpublished).

## C. Beam Monitoring

The exposure was monitored with an argon-filled ionization chamber.[13] The total exposure was $6.24\times10^{11}$ protons delivered over a 24-hour period. A pair of

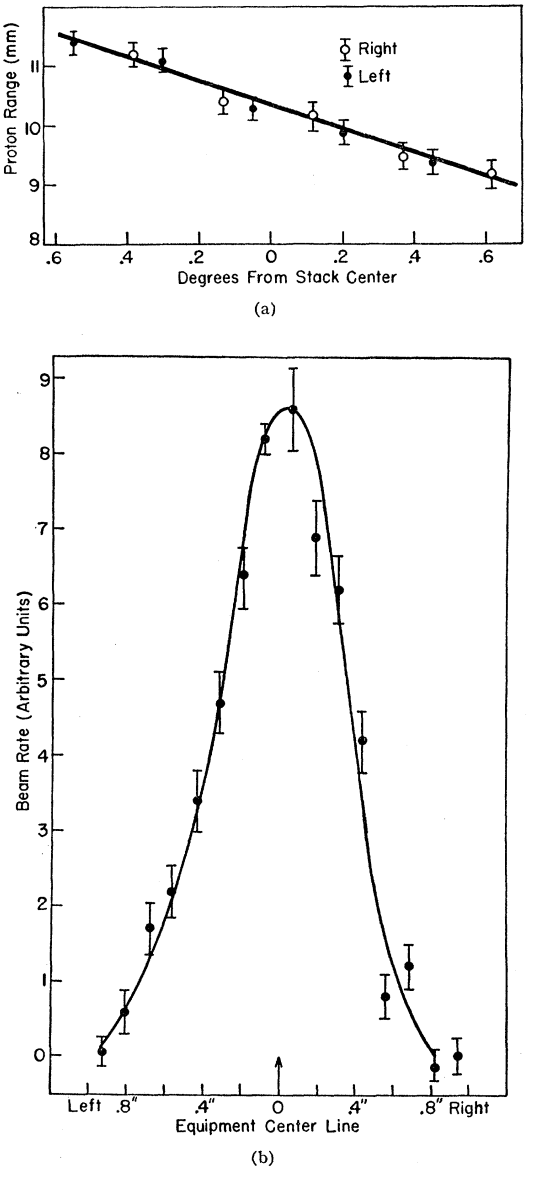


FIG. 4. (a) Variation of range of protons from elastic $p$-$p$ scattering with position of plate in the stack, for both right and left stacks. The horizontal width of the solid line indicates the difference in angular position of the two stacks, as obtained by a least-squares fit. (b) Beam profile obtained by monitoring vertical strips of a nichrome foil activated in the beam during the exposure.

[13] L. G. Pondrom, Phys. Rev. **114**, 1623 (1959).

background stacks was given the same exposure, with the hydrogen target empty.

## III. EMULSION PROCESSING AND SCANNING

### A. Processing

As the emulsions had to be thick to maximize the probability that the muon from the decay of the pion would stop in the same plate as the pion, the emulsions were processed free by the usual variable-temperature technique and alcohol dried. As the processing times required for such thick emulsions might be of some interest to emulsion workers, Table I gives the relevant data. The plates were quite clear, and though slight development and shrinkage gradients were obtained, these were not serious enough to hamper the simple measurements required in this experiment.

### B. Scanning

Only the central areas of the stack were scanned. The author and a scanner each scanned equal areas on both sides; neither was aware at the time of the scanning of the sign of the expected asymmetry, and data sheets were quickly filed. An overlap of about one third in the scanning, randomized so that neither scanner knew he was in a "double-scanned" area, permitted an efficiency check. Over-all efficiency was found to be $0.845\pm0.017$ for the scanner, $0.892\pm0.015$ for the author; no significant variations were found comparing efficiency in right and left stacks and in upper and lower parts of the spectrum, so while the accuracy of the efficiency determination, which rests on the assumption that all events are equally hard to find, may affect the cross-section measurements, it should not affect the asymmetry.

Stopping pions were identified by measuring the ranges of the decay muons; the average range was $600.5\pm3$ microns, with a standard deviation of 34 microns for a single measurement; events were accepted as pions if the "muon" range was between 500 and 700 microns; out of 2927 endings found, 51 were rejected by this criterion.

To minimize range spread due to nuclear scattering, pions were required to be in the forward cone 1 mm back from their stopping point, near the limit of visibility of the track; 106 endings were rejected by this criterion.

Only one half as much area was scanned in the background plates as in the hydrogen exposure plates in order to maximize statistical accuracy per unit scanning time.

The range-energy relationship for the emulsion was determined from the average muon range. Allowing for the apparent shortening of both pion and muon tracks due to multiple scattering,[8] the pion energy was obtained from the values of Barkas *et al.*[14] for emulsion of density 3.815 by multiplying the apparent range by $1.0092\pm0.005$. Corrections were made for energy loss in the target and intervening air space; the average pion energy is determined to an accuracy of $\pm0.3$ Mev at the peak of the spectrum, $\pm0.8$ Mev at the lowest energy observed.

TABLE I. Times used for stages of emulsion processing.[a]

| Stage | Av temp. (°C) | Time |
|---|---|---|
| Detergent pre-soak | 2.7 | 2 hr, 57 min |
| Developer soakup (0.45% Amidol) | 2.7 | 3 hr, 13 min |
| Development | 24.7 | 58 min |
| Acid stop | 5.0 | 4 hr, 4 min |
| Fixing | 10.5 | 8 days |
| (Clearing time was 4½ days) | | |

[a] The emulsions were printed with surface grids to facilitate scanning.

TABLE II. A summary of the events found in the scanning.

| Stack | Events found |
|---|---|
| Right, hydrogen | 1410 |
| Left, hydrogen | 1086 |
| Right, background[a] | 141 |
| Left, background[a] | 128 |

[a] One half as much area scanned as for hydrogen data.

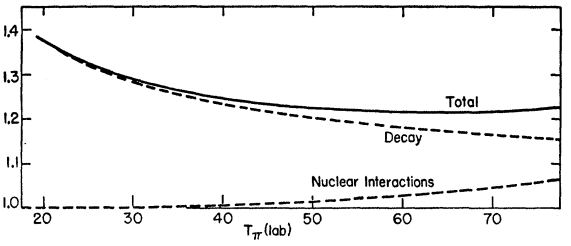


FIG. 5. Correction factors for pion decay and nuclear interaction (capture or back-scattering) used to obtain laboratory cross sections. The solid line gives the product of the two correction factors.

## IV. RESULTS

Table II lists the total number of events found and accepted as stopping positive pions.

Asymmetries can be obtained directly from the raw data, with small corrections for slight differences in the original plate thickness and area scanned. To obtain cross sections, corrections must be made for scanning efficiency (see Sec. III B), muons leaving the plate before stopping (15.8%), and pion decay in flight and nuclear interactions. The latter two corrections are plotted in Fig. 5. The decay correction assumes $\tau_\pi = 2.56\times10^{-8}$ sec,[15] while the nuclear interaction correction is computed from Barkov and Nikol'skii's fit[16] to low-energy pion-nucleus cross sections.

[14] W. H. Barkas, P. H. Barrett, P. Cüer, H. Heckman, F. M. Smith, and H. K. Ticho, Nuovo cimento **8**, 185 (1958).
[15] K. M. Crowe, Nuovo cimento **5**, 541 (1957).
[16] L. M. Barkov and B. A. Nikol'skii, Uspekhi Fiz. Nauk **61**, 341 (1957).

TABLE III. Experimental results; cross sections, asymmetries, and related quantities as a function of pion energy.[a]

| Range in emulsion (mm) | $\bar{T}_\pi$ (lab) | $\bar{T}_\pi$ (c.m.) | $\bar{\theta}_\pi$ (c.m.) | $d^2\sigma/d\Omega dE$ (lab) in microbarns/sr Mev Total | Right | Left | $\frac{d^2\sigma}{d\Omega dE}$ (c.m.) | $\epsilon=\frac{R-L}{R+L}$ | $\frac{\epsilon}{p(\sin\theta)}$ |
|---|---|---|---|---|---|---|---|---|---|
| 63–70 | 76.6 | 66.0 | 99.1° | 0.20±0.13 | 0.15±0.11 | 0.05±0.08 | 0.18±0.12 | 0.120±0.129 | 0.189±0.210 |
| 56–63 | 71.3 | 61.6 | 99.8° | 1.39±0.18 | 0.77±0.14 | 0.62±0.12 | 1.28±0.17 | | |
| 50–56 | 66.3 | 51.4 | 100.5° | 3.45±0.27 | 1.98±0.20 | 1.47±0.17 | 3.17±0.25 | 0.146±0.076 | 0.238±0.124 |
| 45–50 | 62.0 | 53.9 | 101.2° | 2.98±0.27 | 1.89±0.21 | 1.44±0.17 | 3.08±0.25 | 0.136±0.080 | 0.222±0.131 |
| 40–45 | 58.1 | 50.6 | 102.0° | 3.68±0.28 | 2.15±0.21 | 1.53±0.17 | 3.41±0.25 | 0.165±0.072 | 0.270±0.118 |
| 35–40 | 53.9 | 47.4 | 103.0° | 3.01±0.25 | 1.87±0.20 | 1.14±0.16 | 2.80±0.24 | 0.245±0.078 | 0.403±0.128 |
| 30–35 | 49.7 | 44.1 | 104.2° | 1.59±0.23 | 1.01±0.16 | 0.58±0.15 | 1.48±0.21 | 0.272±0.144 | 0.450±0.238 |
| 25–30 | 45.3 | 40.5 | 105.5° | 1.03±0.20 | 0.67±0.14 | 0.36±0.14 | 0.97±0.19 | 0.309±0.177 | 0.514±0.294 |
| 20–25 | 40.6 | 36.8 | 107.0° | 1.12±0.19 | 0.64±0.13 | 0.48±0.13 | 1.06±0.18 | 0.145±0.172 | 0.243±0.288 |
| 15–20 | 35.5 | 32.8 | 108.9° | 0.85±0.17 | 0.41±0.11 | 0.44±0.12 | 0.81±0.16 | −0.028±0.196 | −0.047±0.332 |
| 10–15 | 30.0 | 28.6 | 111.5° | 0.63±0.20 | 0.32±0.11 | 0.31±0.15 | 0.61±0.19 | 0.021±0.311 | 0.036±0.536 |
| 4–10 | 23.1 | 23.4 | 116.3° | 0.56±0.18 | 0.14±0.11 | 0.42±0.13 | 0.56±0.18 | −0.486±0.355 | −0.869±0.635 |

[a] For $T_\pi$(lab) >19 Mev, $d\sigma/d\Omega$(lab) =93±5 μb/sr; $d\sigma/d\Omega$(c.m.) =87±5 μb/sr; $\epsilon=(R-L)/(R+L)$ =0.151±0.021.

The results appear in Table III. Errors quoted for the individual points are statistical only, giving the true relative errors of the points; those quoted for integrated cross sections include additional allowance for errors in the scanning efficiency, monitor calibration, nuclear interaction correction, and range-energy relations.

Sources of energy spread in the pion distribution at the spectrum peak are listed in Table IV. The beam energy spread was measured with the spectrometer and by fitting the Bragg curve,[8] giving values of 6.9 and 7.3 Mev (standard deviation), respectively. Each source is treated as statistically independent of the others and Gaussian. The actual distributions are slightly skewed and have some correlation; for example, a pion low in energy for other reasons will lose more energy in the target. Thus, the actual distribution should be somewhat wider than the value in Table IV and slightly skewed toward low energy. In fitting the data, a Gaussian spread of 6 Mev was assumed.

Allowing for target energy loss, the mean energy of the beam at the center of the target was 417.5 Mev. To simplify the kinematic calculations, it was assumed that the range accurately represented the laboratory momentum of the pion; i.e., that part of the energy spread due to straggling and multiple scattering in the emulsion was neglected. This is the source of the figures for average center-of-mass angle and energy in Table III.

TABLE IV. Sources of energy spread at spectrum peak.

| Source of spread | | Spread (Mev) |
|---|---|---|
| Beam energy spread | | 3.3 |
| Angular spread due to (1.3 Mev/degree): | | |
| Target width | 1.9 Mev | |
| Stack multiple scattering | 0.3 Mev | 2.3 |
| Target and air multiple scattering | 1.25 Mev | |
| Energy loss differences due to: | | |
| Beam width | 0.25 Mev | |
| Path length differences | 1.35 Mev | 1.4 |
| Straggling | | 1.7 |
| Sum assuming statistical independence | | 4.6 |

## V. DISCUSSION

The notation of Rosenfeld[17] will be used throughout the discussion (see caption, Table V).

### A. Cross Sections

The laboratory differential cross section may be compared with values obtained by Fields *et al.*[3] for reaction (1) and Pondrom[13] for reaction (2). Correcting for differences in momentum, these predict, for the given energy and laboratory angle,

$$d\sigma/d\Omega(\pi^+ + d) = 46\pm4 \text{ microbarns/sr},$$

$$\int_{19}^{E_0} dE(d^2\sigma/d\Omega dE)(\pi^+ + n + p) = 44\pm8 \text{ microbarns/sr}$$

giving 90±9 microbarns/sr as compared with the observed 93±5. Pondrom's spectrum (Fig. 6, dotted line), however, does not drop off rapidly enough in energy to fit the observed spectrum; this may be due in part to the large contribution in the low-energy region from the *Ps* and *Pp* isotropic states, both of which are quoted by Pondrom with large errors. As this experiment does not give sufficient data to permit an accurate fit for the six parameters required to specify the spectrum, a restrictive assumption was adopted in an attempt to obtain a better fit. A spectrum of the form $(Sp+0.15Ss+0.2Pp)$, roughly consistent with the data of Fields *et al.* for reaction (2), was assumed. As the range of center-of-mass angles was small, no angular dependence was assumed. This spectrum and a peak for reaction (1), with the experimental resolution folded in, give the fit shown in Fig. 6, with a $\chi^2$ of 16 for 10 degrees of freedom, not unreasonable when the restrictiveness of the assumption and uncertainties in the energy scale are considered.

[17] A. H. Rosenfeld, Phys. Rev. **96**, 139 (1954).

### B. Asymmetry

Rosenfeld[17] gives the results of Marshak and Messiah[1] for the asymmetry in reaction (1) in the form

$$\epsilon \equiv \frac{R-L}{R+L} = \frac{PQA\sin\theta}{A+\cos^2\theta}, \tag{3}$$

where $P$ is the beam polarization and $(A+\cos^2\theta)$ the angular distribution. The asymmetry arises from an interference between $Ss$ and $Ps$ states, with

$$Q = \frac{\sqrt{2}(\eta\eta_c)}{(\eta_c)^2+\eta^2}\sin(\Psi-\tau_1), \tag{4}$$

where $\eta$ is the pion momentum, and the asymmetry is a maximum at

$$\eta_c = \left(\frac{\alpha}{\beta}\right)^{\frac{1}{2}} \frac{(1+|r_1|^2)}{|[r_0+(1/\sqrt{2})]|}, \tag{5}$$

TABLE V. All allowable states with $L\leq 1$ in the reaction $p+p \rightarrow \pi^+ + n + p$. Two-nucleon initial and final states are designated $^{(2S+1)}L_J$ in the conventional manner; the small letter gives the pion angular momentum, its subscript the total $J$ of the final state. $\sigma_{10}$ and $\sigma_{11}$ are the fundamental charge-independent cross sections for total isotopic spin 1, with final nucleon isotopic spin 0, 1, respectively.

| | | | |
|---|---|---|---|
| | Cross section $\sigma_{10}$ | | |
| $(A)$ | $^3P_1$ | $\rightarrow$ | $^3S_1 s_1$ |
| $(B)$ | $^1S_0$ | $\rightarrow$ | $^3S_1 p_0$ |
| $(C)$ | $^1D_2$ | $\rightarrow$ | $^3S_1 p_2$ |
| $(D$–$G)$ | $^3P_{0,1,2}$ or $^3F_2$ | $\rightarrow$ | $^1P_1 p_{0,1,2}$ |
| | Cross section $\sigma_{11}$ | | |
| $(H)$ | $^3P_0$ | $\rightarrow$ | $^1S_0 s_0$ |
| $(I)$ | $^1S_0$ | $\rightarrow$ | $^3P_0 s_0$ |
| $(J)$ | $^1D_2$ | $\rightarrow$ | $^3P_2 p_2$ |
| $(K)$ | $^3P_1$ | $\rightarrow$ | $^3P_0 p_1$ |
| $(L$–$O)$ | $^3P_{0,1,2}$ or $^3F_2$ | $\rightarrow$ | $^3P_1 p_{0,1,2}$ |
| $(P$–$S)$ | $^3P_{1,2}$ or $^3F_{2,3}$ | $\rightarrow$ | $^3P_2 p_{1,2,3}$ |

where $r_0$, $r_1$ are the ratios of the amplitudes of states $B$, $A$ in Table V, relative to that of state $C$, and $\Psi$ and $\tau_1$ are the arguments of $[r_0+(1/\sqrt{2})]$ and $r_1$, respectively. The coefficients $\alpha$, $\beta$ are the $s$- and $p$-wave meson coefficients in the excitation function,

$$\sigma_T = \alpha\eta + \beta\eta^3. \tag{6}$$

The same analysis applies to that part of the cross section for reaction (2) that is contributed by the above-mentioned states. $\mathrm{Sin}(\Psi-\tau_1)$ should be constant by the phenomenological model, and Eq. (4) should contain all momentum dependence of the matrix elements. The contribution of state $(H)$ to reaction (2) is small.

The quantity $\epsilon/P\sin\theta$, which is measured independently of any assumption as to the angular distribution, appears in the last column of Table III and is plotted in Fig. 7.

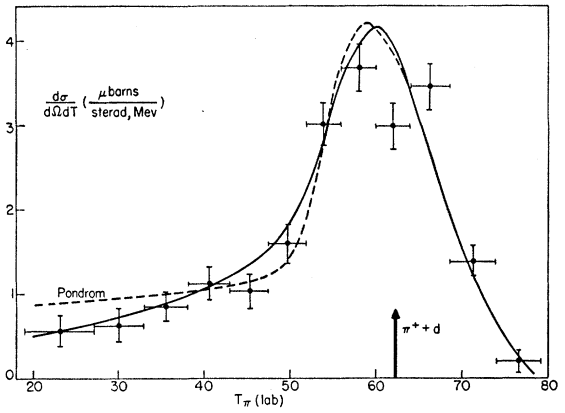


FIG. 6. Laboratory pion spectrum, in microbarns per steradian per Mev. The broken line is obtained by direct computation from the spectrum coefficients of Pondrom. The solid line is fitted by assuming a spectrum of the form $(Sp+0.15Ss+0.2Pp)$. Each curve has the experimental resolution (6 Mev) folded in.

Assuming $\eta_c=0.50$, we obtain values of $\sin(\Psi-\tau_1)$ consistent with those obtained for reaction (1) by other authors[3]:

Please note that the values given are not necessarily those quoted by the authors: They have been recomputed for $\eta_c=0.50$ for comparison with this experiment.

0.55±0.10 This experiment ($\bar{\eta}=0.89$),

0.56±0.05 Crawford and Stevenson, $\pi^+ + d$, ($\eta=0.41$),

0.65±0.10 Fields *et al.*, $\pi^+ + d$, ($\eta=0.97$),

0.53±0.17 McIlwain,[18] $\pi^+ + n + p$ ($\bar{\eta}=0.52$).

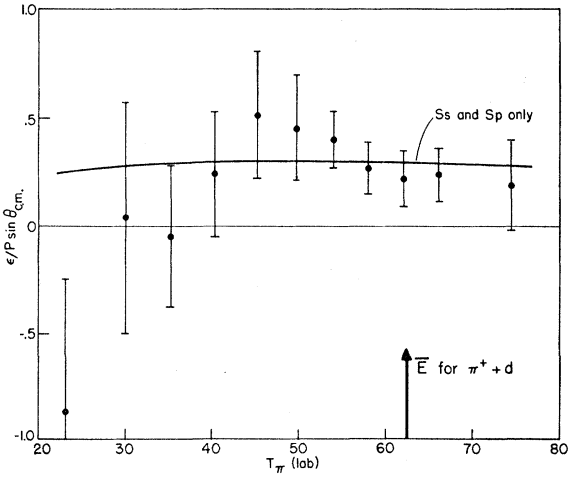


FIG. 7. Energy dependence of $\epsilon/P\sin\theta$. The solid curve is for final nucleon $s$-states only, assuming $\eta_c=0.5$, $\sin(\Psi-\tau_1)=0.56$, $d\sigma/d\Omega$ proportional to $0.40+\cos^2\theta$.

[18] R. L. McIlwain, Thesis, Carnegie Institute of Technology, Pittsburgh, Pennsylvania, 1960 (unpublished).

The value is calculated from the seven highest points in Fig. 7, for which over 98% of the pions should be associated with final nucleon $s$ states. The assumed value of $\eta_c$ gives, with Pondrom's data on the angular distribution, $\alpha/\beta=0.14$, which is the value obtained by Crawford and Stevenson[3] by a fit to the energy dependence of reaction (1).

The curve in Fig. 7 is plotted using this value of $\eta_c$ and Pondrom's value of $A$.

At low energies, the contribution of the spectrum of pions associated with final nuclear $p$ states ($D$–$G$ and $I$–$S$ in Table V) becomes appreciable. Any asymmetry in the angular distribution of pions from these states should be separable from that in equations (3) through (5), as distinct nucleon final states cannot interfere in the angular distribution. Interference is possible, however, within the groups ($D$–$G$) and ($I$–$S$). Thus, as many as 15 matrix elements, and some of their relative phases, may be necessary to specify the asymmetry. No sufficiently detailed data on the low-energy portion of pion production cross sections is available to justify such an analysis, particularly considering the small number of events in this region from this experiment. A study of the reaction $p+p\rightarrow\pi^0+p+p$, which arises exclusively from $\sigma_{11}$, with a polarized beam, would aid in the understanding of this effect. It would appear from the results of this experiment that a small or reversed asymmetry would be expected, as compared with that from reactions (1) and (2).

Assuming the decrease in asymmetry at low energies in Fig. 7 is due to this effect, and using Pondrom's ratio of $p$- to $s$-state nucleon contributions, we can obtain an average value of $\epsilon/P\sin\theta$ for pions associated with nucleon $p$ states, of $-0.37\pm0.35$. The statistics are too poor to justify a more detailed analysis.

After the completion of this work, it was learned that McIlwain[18] has performed a similar measurement with 53% polarized protons at an average bombarding energy of 405 Mev, in somewhat different geometry. He finds $\epsilon=0.199\pm0.055$ for pions centered at 90° in the center-of-mass system, in a broad energy region that might be expected to contain some pions from final nucleon $p$ states. From the results of this experiment, a somewhat lower value of asymmetry would be expected in McIlwain's, but the difference is not statistically significant.

## VI. CONCLUSIONS

Without any detailed analysis, it is clear that the results are qualitatively consistent with the phenomenological theory of meson production. In addition, a reduction of asymmetry at low energy, which may be due to reduced or opposite asymmetry of mesons associated with final nucleon relative $p$ states, seems to be indicated, but this effect would not be sufficient to account for the anomalous result of de Carvalho *et al.*,[4] which would require a reversal of asymmetry involving a major portion of the pion spectrum. Further experimentation, particularly neutral pion production with polarized protons, would clarify this phenomenon.

## ACKNOWLEDGMENTS

The author is deeply indebted to A. V. Crewe and to L. W. Marshall for continuing encouragement and guidance; to U. E. Kruse, C. M. York, V. L. Telegdi, and F. Chilton for valuable suggestions; to R. Levi-Setti for the use of the emulsion laboratory facilities; and to A. Malouhos for diligent and conscientious scanning. S. Marcowitz, B. Ledley, E. Lillethun, and C. Rey helped with the exposure; G. B. March gave valuable assistance in the beam extraction and focussing and the manuscript preparation. The author also wishes to thank Clovis Bordeaux and the cyclotron staff for the excellent machine performance during the run.